

Published in final edited form as:

*Acta Biomater.* 2015 January 1; 11: 204–211. doi:10.1016/j.actbio.2014.09.037.

## Biocompatibility of a Coacervate-Based Controlled Release System for Protein Delivery to the Injured Spinal Cord

Britta M. Rauck<sup>a,b</sup>, Tabitha L. Novosat<sup>c</sup>, Martin Oudega<sup>a,c,d,\*</sup>, and Yadong Wang<sup>a,b,e,f,\*</sup>

<sup>a</sup>Department of Bioengineering, University of Pittsburgh, Pittsburgh, PA, USA

<sup>b</sup>McGowan Institute for Regenerative Medicine, University of Pittsburgh, Pittsburgh, PA, USA

<sup>c</sup>Department of Physical Medicine and Rehabilitation, University of Pittsburgh, Pittsburgh, PA, USA

<sup>d</sup>Department of Neurobiology, University of Pittsburgh, Pittsburgh, PA, USA

<sup>e</sup>Department of Surgery, University of Pittsburgh, Pittsburgh, PA 15219 USA

<sup>f</sup>Department of Chemical and Petroleum Engineering, University of Pittsburgh, Pittsburgh PA 15219, USA

### Abstract

The efficacy of protein-based therapies for treating injured nervous tissue is limited by the short half-life of free proteins in the body. Affinity-based biomaterial delivery systems provide sustained release of proteins, thereby extending the efficacy of such therapies. Here, we investigated the biocompatibility of a novel coacervate delivery system based on poly(ethylene argininy laspartate diglyceride) (PEAD) and heparin in the damaged spinal cord. We found that the presence of the [PEAD:heparin] coacervate did not affect the macrophage response, glial scarring, or nervous tissue loss, which are hallmarks of spinal cord injury. Moreover, the density of axons, including serotonergic axons, at the injury site and the recovery of motor and sensorimotor function were comparable in rats with and without the coacervate. These results revealed the biocompatibility of our delivery system and supported its potential to deliver therapeutic proteins to the injured nervous system.

### Keywords

Spinal cord injury; Growth factor delivery; Biocompatibility; Nervous tissue loss

---

© 2014 Elsevier Ltd. All rights reserved.

\*Corresponding authors: yaw20@pitt.edu, moudega@pitt.edu.

#### Disclosures

The authors declare no conflicts of interest.

**Publisher's Disclaimer:** This is a PDF file of an unedited manuscript that has been accepted for publication. As a service to our customers we are providing this early version of the manuscript. The manuscript will undergo copyediting, typesetting, and review of the resulting proof before it is published in its final citable form. Please note that during the production process errors may be discovered which could affect the content, and all legal disclaimers that apply to the journal pertain.

## 1. Introduction

Endogenous repair of damaged nervous tissue and restoration of motor function is limited following spinal cord injury (SCI) [1]. Administration of therapeutic molecules such as growth factors is one promising strategy to promote repair; however the short half-life of bioactive proteins in vivo limits the efficacy of direct injection [2–6]. Multiple injections or implantation of semi-permanent cannulas may bypass this drawback but require invasive surgical techniques which limit their clinical relevance [7–9]. An injectable, biodegradable, and biocompatible delivery system would provide sustained release of therapeutic proteins, thereby extending their efficacy and avoiding overly invasive delivery methods.

Here, we explored the utility of a unique biodegradable growth factor delivery system for use in the injured spinal cord. The delivery system is composed of a synthetic polycation, poly(ethylene arginylaspartate diglyceride) (PEAD), which is cationic and binds heparin electrostatically [10]. PEAD is biodegradable via hydrolysis of its ester bonds and undergoes approximately 40% degradation over 30 days in vitro [10]. When PEAD and heparin are combined, they interact to form sub-micron (approximately 200 nm) sized liquid droplets that phase-separate from water. The droplet is called a “coacervate”. The liquid coacervate suspension is thus injectable, and sustains the release of heparin-binding growth factors and morphogens with enhanced bioactivity in the skin and heart [11, 12] and has been studied in the context of wound healing, cardiac repair, bone regeneration and therapeutic angiogenesis [13–16]. Protein release from the coacervate can be considered to be a dynamic process, with the ionic environment, the dissociation and re-association of proteins from the coacervate and hydrolytic degradation of PEAD all governing release kinetics. The stronger the interaction between protein and heparin, the slower the release will be.

The coacervate delivery system is composed of a recently-designed polycation and heparin, which due to its anticoagulant properties may potentially exacerbate inflammation and bleeding in damaged nervous tissue. Therefore, we investigated the biocompatibility of the [PEAD:heparin] delivery vehicle in the contused spinal cord of adult rats. Inflammation, glial scarring, nervous tissue loss, and functional impairments are well-documented in this model of SCI, allowing for comprehensive biocompatibility analysis under conditions mimicking clinical neural trauma. In addition, we employed [PEAD:heparin] to administer sonic hedgehog (Shh) to the contused spinal cord as a potential therapeutic strategy [17]. Previously, we have successfully incorporated Shh at 95% loading efficiency into the coacervate and determined that its release is sustained over more than 21 days in vitro, therefore making it a viable candidate for in vivo tissue repair [14].

## 2. Materials and methods

### 2.1 Coacervate preparation

PEAD was synthesized as previously described [10]. PEAD and clinical-grade heparin (Scientific Protein Labs, Waunakee, WI) were each dissolved in 0.9% saline, and sterilized via filtration through 0.22  $\mu\text{m}$  filters. To prepare the coacervate, heparin was complexed with Shh (Peprotech, Rocky Hill, NJ) before PEAD was added. Self-assembly of the PEAD and [heparin:Shh] complexes resulted in immediate phase separation to form the coacervate.

Solutions were prepared at a final Shh concentration of 100 ng/ $\mu$ l. For vehicle controls, heparin was directly complexed with PEAD without the addition of Shh.

## 2.2 Spinal cord contusion model

All animal experiments were conducted in compliance with protocols approved by the Institutional Animal Care and Use Committee at the University of Pittsburgh, with strict adherence to guidelines of the National Institutes of Health and United States Department of Agriculture. Female Sprague Dawley rats (225–250 g, n=10/group; Charles River Laboratory, Wilmington, MA, USA) were anesthetized via intraperitoneal injection of ketamine (60 mg/kg Butlerschein, Dublin, OH, USA) and dexdomitor (0.5 mg/kg, Pfizer, New York, NY, USA). Following laminectomy, an Infinite Horizon impactor (Precision Systems and Instrumentation, LLC, Versailles, KY, USA) was used to generate a 200 kDyne contusion injury at the tenth thoracic segment of the spinal cord. The injury was rinsed with sterile 0.9% saline containing 0.1% gentamicin (VWR, Radnor, PA, USA), the muscles were sutured, and the skin closed with Michel wound clips (Fine Science Tools, Foster City, CA, USA). Three days post-injury, animals were sedated, the injury site was exposed, and the contusion site was injected with 5  $\mu$ l of either [PEAD:Heparin:Shh], [PEAD:Heparin], Shh, or PBS. For rats receiving Shh, the total administered dose was 500 ng.

## 2.3 Post-surgical care

Antisedan (1.5 mg/kg; Pfizer, New York, NY, USA) was injected subcutaneously to wake the animals following procedures. Gentamicin (6 mg/kg; VWR, Radnor, PA, USA) was administered intramuscularly for 7 days post-injury. Rimadyl (5 mg/kg; Pfizer, New York, NY, USA) and Ringer's solution (5 ml; Butlerschein, Dublin, OH, USA) were administered subcutaneously for 6 days post-injury. Bladders were manually expressed twice daily until the ability to urinate was regained (approximately 2 weeks post-injury). All rats were checked at least once a day during the remaining survival time.

## 2.4 Motor function assessment

**2.4.1 Overground walking**—Overground walking ability was assessed using the Basso, Beattie and Bresnahan (BBB) open field test [18] at 1, 3, 7, 14, 21, 28, 35 and 42 days post-injury. Two experimenters blinded to the treatment groups observed the animals for 4 minutes and assigned a score between 0 and 21, with 0 representing complete paralysis and 21 representing normal motor function. BBB scores for each animal were normalized by their 1 day post-injury values and averaged per experimental group.

**2.4.2 Sensorimotor function**—Sensorimotor function was assessed using the horizontal ladder test. Rats were recorded while walking across a ladder with irregularly-spaced rungs. Slips of the foot up to the ankle (small) and whole leg (large) were counted and expressed as a percentage of the total number of steps taken. Three runs were analyzed per animal and averaged per experimental group.

**2.4.3 Gait and footprint**—The DigiGait Analysis System (MouseSpecifics, Boston, MA, USA) was used to analyze hindlimb gait and footprint during locomotion before and after contusion. Animals were acclimated to the treadmill for four days prior to taking baseline

(pre-injury) and endpoint (6 weeks post-injury) measurements at a treadmill speed of 20 cm/s. The videos were then analyzed for paw area, paw angle, and stride length. Endpoint data were expressed relative to baseline data and averaged per experimental group.

## 2.5 Histological procedures and immunocytochemistry

Six weeks post-injury, rats were transcardially perfused with 300 mL PBS, followed by 400 mL 4% paraformaldehyde (Sigma-Aldrich, Allentown, PA, USA) in PBS. Spinal cords were dissected and post-fixed in 4% paraformaldehyde overnight, followed by cryoprotection in 30% sucrose in PBS for at least 48h. A spinal cord segment measuring 12 mm centered on the lesion was cut into serial 14  $\mu$ m-thick cryostat sections. A series of sections was stained with cresyl violet and used for determining spared tissue volume. Other series were immunostained with antibodies against GFAP (1:400, DAKO) to recognize reactive astrocytes, ED1 (1:250, Millipore) to recognize macrophages, 5-HT (1:2000, Immunostar) to detect serotonergic axons, and RT-97 (1:200, DSHB) to detect axons. Briefly, sections were blocked for 1h at room temperature with 10% normal goat serum (NGS) containing 0.1% Triton, then incubated overnight at 4 °C in the primary antibody diluted in 2% NGS with 0.1% Triton. After washing, samples were incubated in the secondary antibody (goat anti-mouse 488 or goat anti-rabbit 594, 1:200, Invitrogen) for 2h at room temperature, washed and counter-stained with DAPI, then coverslipped.

## 2.6 Quantitative immunofluorescence analysis

Images were analyzed using Nikon NIS Elements software. For all immunohistochemical quantification, 4–5 sections centered on the dorsal-ventral axis of the lesion were analyzed and data were averaged per region over all sections. For macrophage quantification, the number of ED1-positive cells was quantified on large image composites of the entire lesion and expressed as a function of the tissue area. Images were taken at 20x and stitched together in order to generate entire lesion images. GFAP intensity was assessed on images taken rostral and caudal to the lesion, as well as at the epicenter. Composite images were obtained that spanned the entire width of the cord at each location. Total intensity was considered to be the average intensity of all regions. The intensities of the 5-HT and RT97 staining were quantified similarly as those of the GFAP staining. The total area of positive axon staining was expressed as a percentage of the analyzed area. The area of interest, intensity and cell counts were quantified in all analyses using NIS Elements.

## 2.7 Statistical Analysis

Data are expressed as mean  $\pm$  standard error of the mean (SEM). Statistical analyses for endpoint outcomes such as Digigait, tissue sparing and staining intensities were performed using one-way ANOVA with Fisher pairwise comparisons when significance ( $p < 0.05$ ) was indicated. Repeated measures analysis was used for time-dependent studies (BBB, horizontal ladder walk) with Fisher pairwise comparisons when significance was indicated. All data were analyzed using Minitab 17 software.

## 3.0 Results

### 3.1 Biocompatibility of the [PEAD:heparin] coacervate

**3.1.1 Effect of the coacervate on inflammation and scarring**—We assessed the biocompatibility of the [PEAD:heparin] coacervate in damaged spinal cord nervous tissue by examining the inflammatory and scarring response. The inflammation response was measured by quantifying the density of ED1-positive macrophages in the lesion epicenter. Macrophages were found to be present in all rats in all four experimental groups. There was no difference in macrophage density in the lesion epicenter between groups ( $p>0.05$ ), suggesting that the presence of the coacervate did not exacerbate inflammation (Figure 1A, D). Scarring was examined by measuring the intensity of GFAP staining surrounding the lesion site. In all rats in all groups, scarring was found to be present. Quantification showed similar intensities between groups ( $p>0.05$ ), indicating that the delivery vehicle did not aggravate glial scarring beyond what is normally observed in the contused spinal cord (Figure 1B, C, D).

**3.1.2 Nervous tissue and axon loss**—To study the effect of the presence of the [PEAD:heparin] coacervate on tissue loss, the volume of spared nervous tissue was quantified stereologically. Figure 2 shows the nervous tissue volume expressed as a percentage of a comparable segment of uninjured healthy spinal cord tissue. The data showed that the coacervate does not aggravate tissue loss beyond what is normally observed after a contusion injury. There were no statistically significant differences between groups.

To study the effect of the presence of the [PEAD:heparin] coacervate on axon loss, axonal density was quantified using RT97 staining to detect axons in general, and 5-HT to specifically detect serotonergic axons. Analysis of axon density revealed that the presence of the coacervate did not affect the axonal (general or serotonergic) density either rostral or caudal to the lesion (Figure 3, 4).

**3.1.3 Motor function assessment**—Overground walking ability was assessed weekly using the BBB open field test. (Figure 5). There were no statistical differences between the control and experimental groups, indicating that the coacervate did not negatively affect recovery of overground walking. Hindlimb sensorimotor function was assessed using the horizontal ladder test. The results showed that the presence of the [PEAD:heparin] coacervate did not affect hindlimb sensorimotor function (Figure 6). Gait-related aspects of locomotion were examined using treadmill walking in a Digigait. Our data revealed comparable outcomes between delivery vehicle and control groups (Figure 7). In both the PBS control and coacervate alone groups, 10% and 20% of animals, respectively, were incapable of treadmill walking at 20 cm/s. Stride length was also comparable between treatment and control groups; injured animals adopt a longer stride length as it takes more time for them to lift and swing the hindlimb through to the top of the step. Paw angle was also similar in the delivery vehicle and PBS group. The increased paw angle is a result of attempted stability following injury. Hindlimb weakness prevents the animals from adopting a normal stance and thus their paws turn out in order to provide more stability. As the

hindlimb stability improves, paw angle will decrease. Together the data showed that gait-related aspects of overground walking are not affected by the coacervate.

### 3.2 Effect of Shh released from coacervate

Rats that received Shh-coacervate exhibited a significant reduction in glial scarring in the contused spinal cord segment as well as at the lesion epicenter compared to the PBS and coacervate-only groups (Figure 1B, C). Rats receiving free Shh also exhibited significantly less scarring at the lesion epicenter compared with empty coacervate groups.

We did not observe a significant increase in tissue sparing between groups; however the Shh-coacervate group had the largest percentage of spared tissue, suggesting a potential effect of Shh delivery on tissue preservation (Figure 2). Similarly, there appeared to be trends towards increased staining for axons in general and serotonergic axons in particular in the Shh-coacervate group, which was most prominently observed in the spinal cord just rostral to the lesion (Figure 3), though these results were not statistically significant.

All rats in the free Shh and Shh-coacervate groups were physically capable of walking on the treadmill at a speed of 20 cm/s. In the empty coacervate and PBS control groups, 20% and 10% of animals, respectively, were unable to walk and therefore data could not be obtained. These results showed that animals receiving Shh performed better at the used walking speed than animals receiving control injections. Additionally, stride length was measured and compared with that of healthy animals. In Shh-coacervate rats the stride length was not significantly different from healthy uninjured rats. Shh-coacervate and free Shh animals had a significantly lower paw angle than PBS or empty coacervate groups, though these values were still significantly larger than the paw angle of healthy animals. The significant reduction seen in rats receiving Shh suggested an increased stability in overground walking.

## 4.0 Discussion

Damage to the spinal cord characteristically causes inflammation, glial scarring, nervous tissue and axon loss, and functional impairments [19, 20]. Sustained delivery of therapeutic proteins using biomaterials may support tissue repair and functional restoration. However, the introduction of a foreign material may exacerbate the typical responses to injury thereby further obstructing natural and treatment-mediated repair. Here we sought to determine the biocompatibility of a coacervate-based drug delivery system in damaged nervous tissue using an adult rat model of contusive SCI. Because the delivery system is composed of heparin, a known anticoagulant, and PEAD, a polycation, we aimed to investigate its effect on the destructive events which naturally occur following traumatic SCI. PEAD is an arginine-based polyester; therefore we hypothesized that it overcomes the typical biocompatibility issues encountered with synthetic polycations [10]. Previously, *in vitro* cytocompatibility studies with NIH 3T3 fibroblasts and human aortic endothelial cells demonstrated that PEAD exhibited no toxicity at a concentration of 1 mg/ml, a concentration which is 100 times higher than that which is used for the polycation polyethylenimine. Our results indicated that the coacervate did not affect the inflammatory response, glial scarring, nervous tissue loss, axonal loss, or motor and sensorimotor



impairment beyond what is normally observed after spinal cord contusion. These anatomical and functional outcomes suggest that the [PEAD:heparin] coacervate is safe for delivery of therapeutic proteins to the injured spinal cord.

Following contusive spinal cord injury, macrophages and activated microglia invade the epicenter and surrounding tissue as part of the injury-induced inflammatory response [21]. These macrophages are involved in the clearance of debris from the injury site, but also contribute to further neural cell death by secreting reactive oxygen species and proinflammatory cytokines [22–24]. We found that the [PEAD:heparin] coacervate did not affect the number of ED1-positive cells in the contused spinal cord segment, suggesting that the material does not elevate the response in nearby nervous tissue nor attract additional blood-borne monocytes to the damaged tissue.

Glial scar formation around the injury epicenter is a well-characterized response to spinal cord injury. The scar composed of several cell types, including reactive, GFAP-expressing astrocytes which secrete growth-inhibitory molecules that obstruct endogenous and treatment-induced axon elongation [25]. The degree of scarring is correlated with the lack of spontaneous recovery and the inefficacy of repair strategies based on axonal regeneration/sprouting [26]. Our data showed that the [PEAD:heparin] coacervate did not lead to intensified GFAP staining (i.e., aggravated glial scarring) in the contused spinal cord segment, suggesting that the coacervate did not further exacerbate the astrocytic reaction to the injury, or attract more astrocytes to the lesion.

The forces generated during a contusive impact to the spinal cord leads to immediate neural cell death, followed by an extended period of progressive cell death and tissue removal. Ultimately, one or more fluid-filled cystic cavities appear at the site of the injury. We observed that the presence of the [PEAD:heparin] coacervate did not lead to increased nervous tissue loss in the contused spinal cord segment. Moreover, our data showed that the number of axons, including serotonergic axons, was similar in rats with or without the [PEAD:heparin] coacervate. This observation may be related to the finding that the coacervate does not evoke further nervous tissue loss beyond what is typically observed after a spinal cord contusion. The importance of the serotonergic axons lies in their involvement in the initiation and modulation of locomotor activities, in part through their role in the central pattern generator [27–29]. Likewise, motor function outcomes were comparable between experimental groups in this study, indicating that the presence of the coacervate did not worsen functional impairment, an observation which is consistent with studies linking the degree of nervous tissue sparing with functional outcomes [30–33]. Taken together, these findings support the potential of the [PEAD:heparin] coacervate for delivery of therapeutics to the damaged spinal cord.

An added objective of our study was to examine the effects of Shh released by the [PEAD:heparin] coacervate. Shh was chosen as a model protein because of its involvement in various cellular events that may occur during nervous tissue repair [17, 34–37]. A few studies have indicated the potential for exogenous Shh administration to influence outcomes following CNS trauma. Treatment with Shh was shown to induce host cell response following SCI and stroke in rats [38–40] and to decrease glial scarring and improve

functional recovery in both contusion and dorsal over-hemisection models of SCI in mice [41]. The precise mechanisms underlying these Shh-mediated effects are unclear. We found a reduction in GFAP intensity in Shh-injected rats, suggesting that Shh may play a role in reducing astrocyte activation and subsequent scar formation. While the mechanism of Shh effects on glial scar formation has not been explicitly studied, it has been reported that hedgehog pathway activation in astrocytes can alter their phenotypic behavior following injury [42]. Therefore it is possible that exogenous Shh administration reduces activated astrocytes' contribution to scar formation. This hypothesis would need to be confirmed in future mechanistic studies.

We observed statistically non-significant trends toward functional recovery, axon density, and tissue sparing in Shh-coacervate groups. Possibly, the dose of Shh was insufficient to exert a biologically significant effect. At present, there are few published studies using exogenous Shh in SCI models; therefore, we chose 500 ng Shh based on precedent combined with the dose that was demonstrated to elicit a significant response in cardiac cells in vitro [14]. An alternative explanation for the trends is that a 3-day delayed injection, while clinically relevant, is unsuitable for growth factor administration. The increasing inflammatory response during this time delay may have accelerated Shh release from the coacervate or degraded the coacervate more rapidly than expected. While the stability of the coacervate in vivo has yet to be fully studied, a recent investigation performed in a model of myocardial infarction (MI) suggests that the coacervate persists for at least several days post-injection [43]. In that study, rhodamine-labeled BSA was injected with or without coacervate delivery and at 3 days post-injection, there was strong fluorescence labeling in the injection site in the coacervate group, and no fluorescence labeling in the groups which received free BSA. This study suggested that the coacervate is effective at protecting its contents in a highly inflammatory environment in the short-term, and that that persistence is capable of translating in to long term effects such as lower inflammation, fibrosis, and myocardial cell death following MI. In the spinal cord injury model, also a highly inflammatory environment, it is likely that the injected coacervate demonstrates a similar ability to protect its contents and sustain the release of heparin-binding proteins; however the lack of any significant effect of Shh delivery in this study indicates that the current treatment strategy will need to be adjusted. Future experiments will need to optimize dose and treatment time for Shh delivery to the contused spinal cord to foster biologically significant anatomical repair and functional recovery.

## 5.0 Conclusion

The present work demonstrated the utility of an injectable, affinity-based growth factor delivery system to the injured spinal cord. The [PEAD:heparin] coacervate is compatible with spinal cord nervous tissue and does not negatively impact the typical course of injury progression. Controlled release of Shh resulted in decreased glial scarring, and may have positive effects on neuronal survival and nervous tissue sparing. Future work will focus on dosage optimization and combinatorial approaches, such as multiple growth factor delivery, or cell transplantation combined with growth factor therapy.



## Acknowledgments

The authors are deeply thankful to Callen Wallace in the Center for Biological Imaging at the University of Pittsburgh for assistance in automated image analysis, and Mr. Lou Johnson for statistical consulting. Funding for this work was generously provided by NIH 2T32EB003392-07 and NSF DMR-1206589.

## References

1. Gamera C, Rauck B, Wang Y. Materials for central nervous system regeneration: bioactive cues. *Journal of Materials Chemistry*. 2011; 21:7033–51.
2. Mocchetti I, Wrathall JR. Neurotrophic factors in central nervous system trauma. *J Neurotrauma*. 1995; 12:853–70. [PubMed: 8594213]
3. Sayer FT, Oudega M, Hagg T. Neurotrophins reduce degeneration of injured ascending sensory and corticospinal motor axons in adult rat spinal cord. *Exp Neurol*. 2002; 175:282–96. [PubMed: 12009779]
4. McTigue DM, Horner PJ, Stokes BT, Gage FH. Neurotrophin-3 and brain-derived neurotrophic factor induce oligodendrocyte proliferation and myelination of regenerating axons in the contused adult rat spinal cord. *The Journal of neuroscience: the official journal of the Society for Neuroscience*. 1998; 18:5354–65. [PubMed: 9651218]
5. Bamber NI, Li H, Lu X, Oudega M, Aebischer P, Xu XM. Neurotrophins BDNF and NT-3 promote axonal re-entry into the distal host spinal cord through Schwann cell-seeded mini-channels. *Eur J Neurosci*. 2001; 13:257–68. [PubMed: 11168530]
6. Bregman BS, McAtee M, Dai HN, Kuhn PL. Neurotrophic factors increase axonal growth after spinal cord injury and transplantation in the adult rat. *Exp Neurol*. 1997; 148:475–94. [PubMed: 9417827]
7. Mantilla CB, Gransee HM, Zhan WZ, Sieck GC. Motoneuron BDNF/TrkB signaling enhances functional recovery after cervical spinal cord injury. *Exp Neurol*. 2013; 247:101–9. [PubMed: 23583688]
8. Xu XM, Guenard V, Kleitman N, Aebischer P, Bunge MB. A combination of BDNF and NT-3 promotes supraspinal axonal regeneration into Schwann cell grafts in adult rat thoracic spinal cord. *Exp Neurol*. 1995; 134:261–72. [PubMed: 7556546]
9. Parr AM, Tator CH. Intrathecal epidermal growth factor and fibroblast growth factor-2 exacerbate meningeal proliferative lesions associated with intrathecal catheters. *Neurosurgery*. 2007; 60:926–33. discussion -33. [PubMed: 17460529]
10. Chu H, Gao J, Wang Y. Design, synthesis, and biocompatibility of an arginine-based polyester. *Biotechnol Prog*. 2012; 28:257–64. [PubMed: 22034156]
11. Chu H, Johnson NR, Mason NS, Wang Y. A [polycation:heparin] complex releases growth factors with enhanced bioactivity. *J Control Release*. 2011; 150:157–63. [PubMed: 21118705]
12. Zern BJ, Chu H, Wang Y. Control growth factor release using a self-assembled [polycation:heparin] complex. *PloS one*. 2010; 5:e11017. [PubMed: 20543985]
13. Johnson NR, Wang Y. Controlled delivery of heparin-binding EGF-like growth factor yields fast and comprehensive wound healing. *J Control Release*. 2013; 166:124–9. [PubMed: 23154193]
14. Johnson NR, Wang Y. Controlled delivery of sonic hedgehog morphogen and its potential for cardiac repair. *PloS one*. 2013; 8:e63075. [PubMed: 23690982]
15. Li H, Johnson NR, Usas A, Lu A, Poddar M, Wang Y, et al. Sustained Release of Bone Morphogenetic Protein 2 via Coacervate Improves the Osteogenic Potential of Muscle-Derived Stem Cells. *Stem Cells Translational Medicine*. 2013; 2:667–77. [PubMed: 23884640]
16. Chu H, Gao J, Chen C-W, Huard J, Wang Y. Injectable fibroblast growth factor-2 coacervate for persistent angiogenesis. *Proceedings of the National Academy of Sciences*. 2011; 108:13444–9.
17. Marti E, Bovolenta P. Sonic hedgehog in CNS development: one signal, multiple outputs. *Trends Neurosci*. 2002; 25:89–96. [PubMed: 11814561]
18. Basso DM, Beattie MS, Bresnahan JC. A sensitive and reliable locomotor rating scale for open field testing in rats. *Journal of neurotrauma*. 1995; 12:1–21. [PubMed: 7783230]

19. Hagg T, Oudega M. Degenerative and spontaneous regenerative processes after spinal cord injury. *J Neurotrauma*. 2006; 23:264–80. [PubMed: 16629615]
20. Fitch MT, Doller C, Combs CK, Landreth GE, Silver J. Cellular and Molecular Mechanisms of Glial Scarring and Progressive Cavitation: In Vivo and In Vitro Analysis of Inflammation-Induced Secondary Injury after CNS Trauma. *The Journal of Neuroscience*. 1999; 19:8182–98. [PubMed: 10493720]
21. Leskovaara A, Moriarty LJ, Turek JJ, Schoenlein IA, Borgens RB. The macrophage in acute neural injury: changes in cell numbers over time and levels of cytokine production in mammalian central and peripheral nervous systems. *J Exp Biol*. 2000; 203:1783–95. [PubMed: 10821736]
22. Kigerl KA, Ankeny DP, Garg SK, Wei P, Guan Z, Lai W, et al. System xc<sup>-</sup> regulates microglia and macrophage glutamate excitotoxicity in vivo. *Experimental Neurology*. 2012; 233:333–41. [PubMed: 22079587]
23. Kigerl KA, Gensel JC, Ankeny DP, Alexander JK, Donnelly DJ, Popovich PG. Identification of two distinct macrophage subsets with divergent effects causing either neurotoxicity or regeneration in the injured mouse spinal cord. *The Journal of neuroscience: the official journal of the Society for Neuroscience*. 2009; 29:13435–44. [PubMed: 19864556]
24. Hausmann ON. Post-traumatic inflammation following spinal cord injury. *Spinal Cord*. 2003; 41:369–78. [PubMed: 12815368]
25. Fawcett JW, Asher RA. The glial scar and central nervous system repair. *Brain Res Bull*. 1999; 49:377–91. [PubMed: 10483914]
26. Fitch MT, Silver J. CNS injury, glial scars, and inflammation: Inhibitory extracellular matrices and regeneration failure. *Exp Neurol*. 2008; 209:294–301. [PubMed: 17617407]
27. Nishimaru H, Takizawa H, Kudo N. 5-Hydroxytryptamine-induced locomotor rhythm in the neonatal mouse spinal cord in vitro. *Neuroscience letters*. 2000; 280:187–90. [PubMed: 10675792]
28. Cazalets JR, Sqalli-Houssaini Y, Clarac F. Activation of the central pattern generators for locomotion by serotonin and excitatory amino acids in neonatal rat. *The Journal of physiology*. 1992; 455:187–204. [PubMed: 1362441]
29. Takeoka A, Kubasak MD, Zhong H, Roy RR, Phelps PE. Serotonergic innervation of the caudal spinal stump in rats after complete spinal transection: Effect of olfactory ensheathing glia. *The Journal of Comparative Neurology*. 2009; 515:664–76. [PubMed: 19496067]
30. Ritfeld GJ, Nandoe Tewarie RDS, Vajn K, Rahiem ST, Hurtado A, Wendell DF, et al. Bone Marrow Stromal Cell-Mediated Tissue Sparing Enhances Functional Repair After Spinal Cord Contusion in Adult Rats. *Cell Transplantation*. 2012; 21:1561–75. [PubMed: 22526408]
31. Ritfeld GJ, Rauck BM, Novosat TL, Park D, Patel P, Roos RA, et al. The effect of a polyurethane-based reverse thermal gel on bone marrow stromal cell transplant survival and spinal cord repair. *Biomaterials*. 2014; 35:1924–31. [PubMed: 24331711]
32. Rabchevsky AG, Fugaccia I, Fletcher-Turner A, Blades DA, Mattson MP, Scheff SW. Basic fibroblast growth factor (bFGF) enhances tissue sparing and functional recovery following moderate spinal cord injury. *J Neurotrauma*. 1999; 16:817–30. [PubMed: 10521141]
33. Basso DM. Neuroanatomical substrates of functional recovery after experimental spinal cord injury: implications of basic science research for human spinal cord injury. *Physical therapy*. 2000; 80:808–17. [PubMed: 10911417]
34. Alvarez JI, Dodelet-Devillers A, Kebir H, Ifergan I, Fabre PJ, Terouz S, et al. The Hedgehog pathway promotes blood-brain barrier integrity and CNS immune quiescence. *Science*. 2011; 334:1727–31. [PubMed: 22144466]
35. Straface G, Aprahamian T, Flex A, Gaetani E, Biscetti F, Smith RC, et al. Sonic hedgehog regulates angiogenesis and myogenesis during post-natal skeletal muscle regeneration. *Journal of cellular and molecular medicine*. 2009; 13:2424–35. [PubMed: 18662193]
36. Lai K, Kaspar BK, Gage FH, Schaffer DV. Sonic hedgehog regulates adult neural progenitor proliferation in vitro and in vivo. *Nature neuroscience*. 2003; 6:21–7.
37. Hashimoto M, Ishii K, Nakamura Y, Watabe K, Kohsaka S, Akazawa C. Neuroprotective effect of sonic hedgehog up-regulated in Schwann cells following sciatic nerve injury. *J Neurochem*. 2008; 107:918–27. [PubMed: 18786173]

38. Bambakidis NC, Petrullis M, Kui X, Rothstein B, Karampelas I, Kuang Y, et al. Improvement of neurological recovery and stimulation of neural progenitor cell proliferation by intrathecal administration of Sonic hedgehog. *Journal of neurosurgery*. 2012; 116:1114–20. [PubMed: 22324418]
39. Bambakidis NC, Wang RZ, Franic L, Miller RH. Sonic hedgehog-induced neural precursor proliferation after adult rodent spinal cord injury. *Journal of neurosurgery*. 2003; 99:70–5. [PubMed: 12859063]
40. Bambakidis NC, Horn EM, Nakaji P, Theodore N, Bless E, Dellovade T, et al. Endogenous stem cell proliferation induced by intravenous hedgehog agonist administration after contusion in the adult rat spinal cord. *J Neurosurg Spine*. 2009; 10:171–6. [PubMed: 19278333]
41. Lowry N, Goderie SK, Lederman P, Charniga C, Gooch MR, Gracey KD, et al. The effect of long-term release of Shh from implanted biodegradable microspheres on recovery from spinal cord injury in mice. *Biomaterials*. 2012; 33:2892–901. [PubMed: 22243800]
42. Sirko S, Behrendt G, Johansson PA, Tripathi P, Costa M, Bek S, et al. Reactive glia in the injured brain acquire stem cell properties in response to sonic hedgehog. [corrected]. *Cell stem cell*. 2013; 12:426–39. [PubMed: 23561443]
43. Chu H, Chen C-W, Huard J, Wang Y. The effect of a heparin-based coacervate of fibroblast growth factor-2 on scarring in the infarcted myocardium. *Biomaterials*. 2013; 34:1747–56. [PubMed: 23211448]

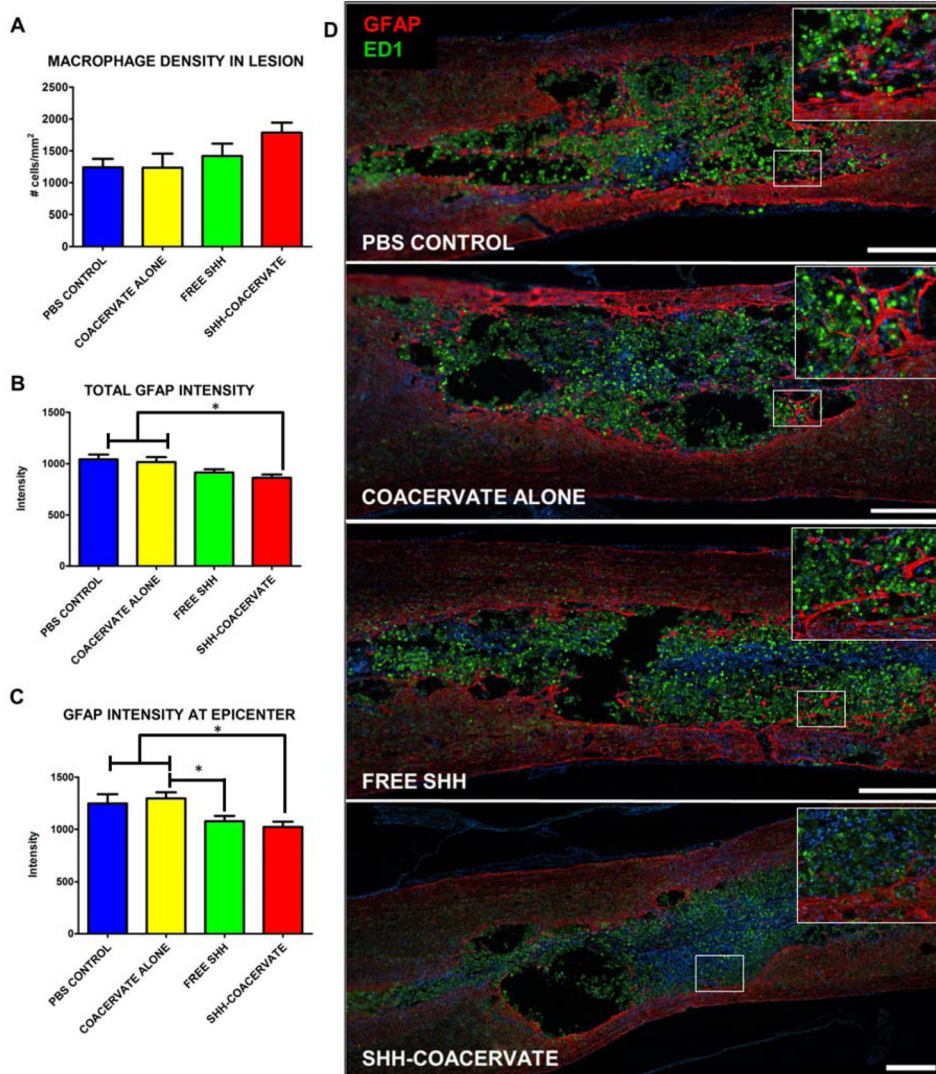


**Figure 1. Effect of [PEAD:heparin] on the inflammatory response**

The coacervate does not increase the macrophage density at the lesion epicenter (A, D). Glial scarring, as measured by the intensity of GFAP staining, was also not different in groups receiving the coacervate compared to PBS controls. The intensity of the entire glial scar was quantified (B) as well as at the lesion epicenter, where presumably scarring would be the most prominent (C). In both cases, animals receiving the Shh coacervate had a significant ( $p < 0.05$ ) reduction in GFAP intensity compared to PBS and empty coacervate groups, indicating a possible effect of Shh delivery on scar formation. (Scale bar = 500  $\mu\text{m}$ ).

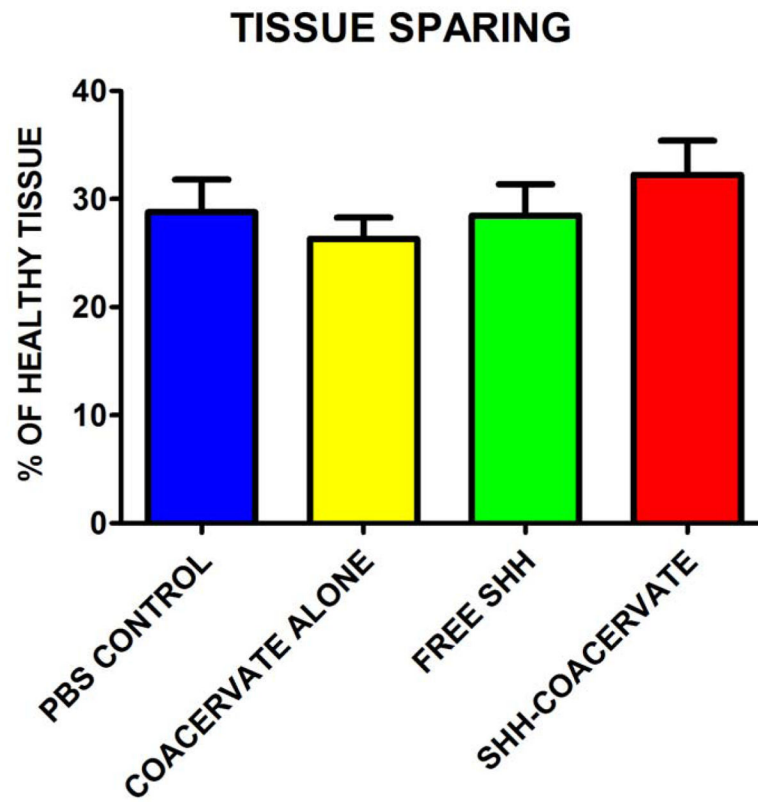


**Figure 2. Effect of coacervate administration on nervous tissue sparing**  
Nervous tissue sparing was not statistically significant between experimental groups; however Shh-coacervate treatment did result in the largest percentage of tissue sparing.

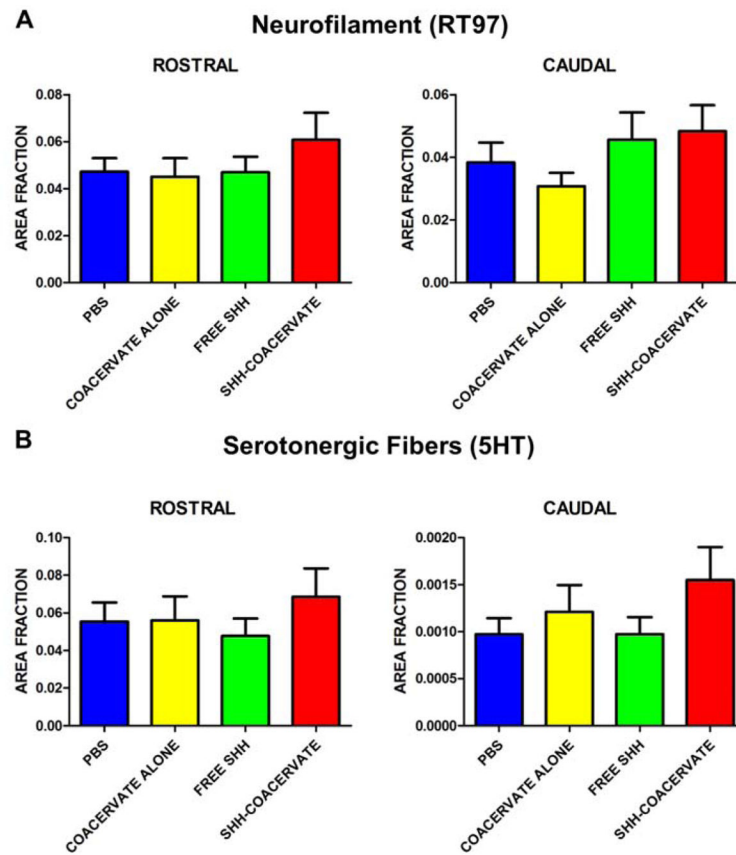


**Figure 3. Density of axons and serotonergic fibers rostral and caudal to the lesion**  
 The amount of positive neurofilament (A) and serotonergic fiber (B) staining was determined by calculating the area of positive staining as a fraction of total tissue area.



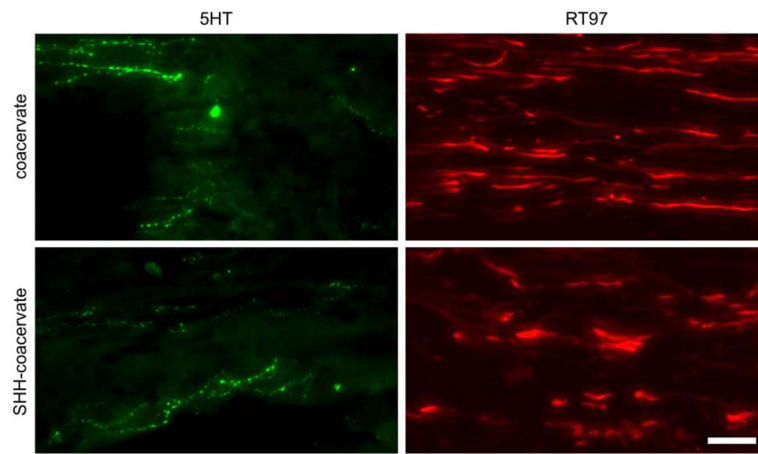


**Figure 4. Axons and serotonergic fiber growth was similar across groups**  
Shh delivery did not significantly increase the amount of 5HT- or RT97-positive fibers.  
Representative images of axon growth are shown just caudal to the lesion site. Scale bar: 75  $\mu\text{m}$ .

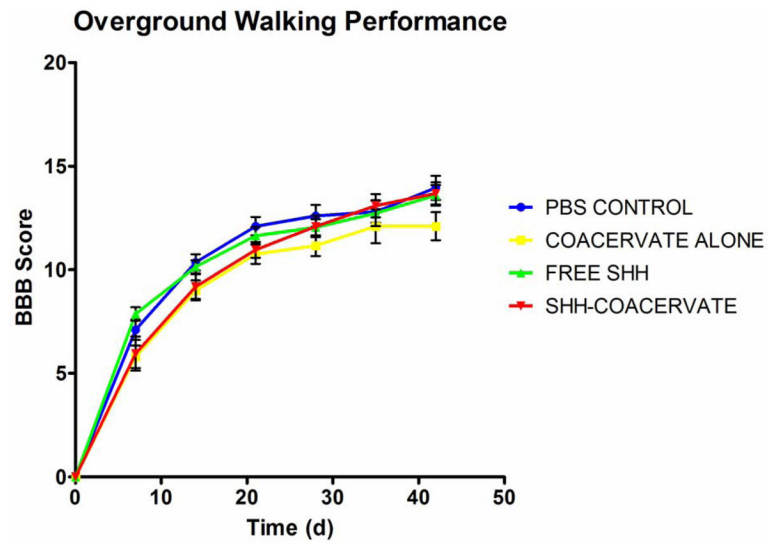


**Figure 5. The coacervate did not impact BBB outcomes**

While no differences were observed between groups, free Shh rats performed well early, whereas Shh-coacervate groups had steadily increasing BBB scores throughout the study.

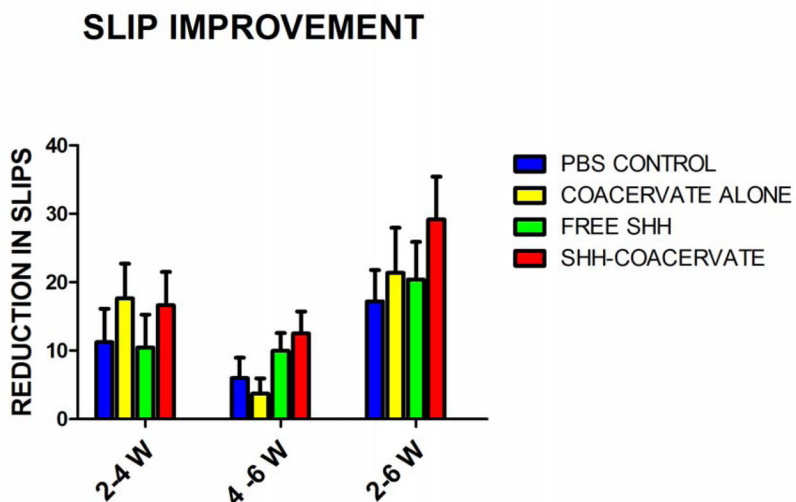


**Figure 6. Improvement in hindlimb stepping over time**

There were no significant differences in sensorimotor recovery between groups. Shh-coacervate groups had the largest decrease in the number of slips made over the time course of the study period, indicating a potential effect of Shh delivery on sensorimotor recovery.

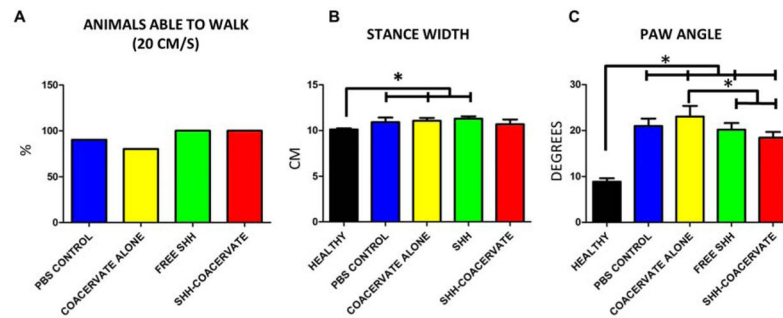


**Figure 7. Gait analysis reveals slight improvements in overground walking ability of Shh-coacervate animals**

In control groups, three animals were unable to walk at the recording speed of 20 cm/s. All animals in free Shh and Shh-coacervate groups were capable of walking (A). The stride length of Shh-coacervate animals was not significantly different than healthy animals, suggesting an improvement in stepping (B). The paw angle of free Shh and Shh-coacervate animals was significantly less than in controls, suggesting an improved stability when stepping, though the paw angles were still significantly different than in uninjured controls (C).